

# Variability in Cardiac miRNA-122 Level Determines Therapeutic Potential of miRNA-Regulated AAV Vectors

Izabela Kraszewska,<sup>1</sup> Mateusz Tomczyk,<sup>1</sup> Kalina Andrysiak,<sup>1</sup> Monika Biniecka,<sup>2</sup> Anja Geisler,<sup>3</sup> Henry Fechner,<sup>3</sup> Michał Zembala,<sup>4</sup> Jacek Stępniewski,<sup>1</sup> Józef Dulak,<sup>1,2</sup> and Agnieszka Jaźwa-Kusior<sup>1</sup>

<sup>1</sup>Department of Medical Biotechnology, Faculty of Biochemistry, Biophysics and Biotechnology, Jagiellonian University, 30-387 Kraków, Poland; <sup>2</sup>Kardio-Med Silesia, 41-800 Zabrze, Poland; <sup>3</sup>Department of Applied Biochemistry, Institute of Biotechnology, Technische Universität Berlin, 13355 Berlin, Germany; <sup>4</sup>Department of Cardiac Surgery, Heart and Lung Transplantation and Mechanical Circulatory Support, Silesian Center for Heart Diseases, 41-800 Zabrze, Poland

**Systemically delivered adeno-associated viral vector serotype 9 (AAV9) effectively transduces murine heart, but provides transgene expression also in liver and skeletal muscles. Improvement of the selectivity of transgene expression can be achieved through incorporation of target sites (TSs) for miRNA-122 and miRNA-206 into the 3' untranslated region (3' UTR) of the expression cassette. Here, we aimed to generate such miRNA-122- and miRNA-206-regulated AAV9 vector for a therapeutic, heart-specific overexpression of heme oxygenase-1 (HO-1). We successfully validated the vector functionality in murine cell lines corresponding to tissues targeted by AAV9. Next, we evaluated biodistribution of transgene expression following systemic vector delivery to HO-1-deficient mice of mixed C57BL/6J × FVB genetic background. Although AAV genomes were present in the hearts of these animals, HO-1 protein expression was either absent or significantly impaired. We found that miRNA-122, earlier described as liver specific, was present also in the hearts of C57BL/6J × FVB mice. Various levels of miRNA-122 expression were observed in the hearts of other mouse strains, in heart tissues of patients with cardiomyopathy, and in human induced pluripotent stem cell-derived cardiomyocytes in which we also confirmed such posttranscriptional regulation of transgene expression. Our data clearly indicate that therapeutic utilization of miRNA-based regulation strategy needs to consider inter-individual variability.**

## INTRODUCTION

Nowadays, gene therapy is gradually emerging as one of the most powerful strategies in the treatment of numerous inherited and acquired disorders, including hemophilia, spinal muscular atrophy, or Leber's hereditary optic neuropathy (reviewed in Wang et al.<sup>1</sup>). Even though various transgene delivery methods were developed, it appears that vectors based on adeno-associated viruses (AAVs) are the most successful so far, providing high expression of the therapeutic gene with very limited immune response in the host organism.<sup>2</sup> Still, the development of a therapy restricted to the selected organ or cell type remains challenging in many cases. Although partial

selectivity of the expression can be obtained through the utilization of appropriate AAV serotype with tropism toward particular tissues,<sup>3</sup> it is not sufficient to prevent all off-target effects associated with the systemic delivery of the vector. Novel approaches aiming to overcome this issue focus on the engineering of cell-type-specific AAV capsids using directed evolution strategy; however, generation of such novel vectors with sufficiently high infectivity is very laborious and problematic in terms of specificity toward given cells and species.<sup>4</sup> Sometimes it is possible to administer the vector directly to the chosen tissue, i.e., into the cardiac muscle using a catheter-based electro-mechanical mapping and injection (NOGA) system.<sup>5</sup> Nevertheless, this route of delivery is invasive and can be hazardous to the patient, especially considering coexisting disorders. Thus, the most desirable cardiac gene therapy vector would be infused intravenously and show efficient and selective gene transfer to the heart.

The majority of cardiac-muscle-targeting vectors are based on AAV serotype 9 (AAV9) because it is the most efficient vector in *in vivo* applications with described tropism toward murine heart, skeletal muscles, and liver following systemic administration.<sup>6</sup> Thus, in order to further improve the vector properties and increase its cardiac specificity, additional regulatory mechanisms should be introduced. Unfortunately, incorporation of heart-specific promoters such as alpha myosin heavy chain ( $\alpha$ -MHC),<sup>7</sup> myosin light chains (MLC2v),<sup>8</sup> and cardiac troponin T (cTnT)<sup>9</sup> into the expression cassette does not prevent vector leakage and transgene expression in other transduced tissues, e.g., skeletal muscles or liver.<sup>10,11</sup> Other shortcomings of such a strategy may include a decreased level of transgene expression as compared with the strong promoters of viral origin like cytomegalovirus (CMV).<sup>11</sup> Hybrid promoters consisting of parts of CMV and eukaryotic promoters may help to overcome this issue; but on the other

Received 18 February 2020; accepted 7 May 2020;  
<https://doi.org/10.1016/j.omtm.2020.05.006>.

**Correspondence:** Agnieszka Jaźwa-Kusior, PhD, Department of Medical Biotechnology, Faculty of Biochemistry, Biophysics and Biotechnology, Jagiellonian University, Gronostajowa Str. 7, 30-387 Kraków, Poland.  
**E-mail:** [agnieszka.jazwa@uj.edu.pl](mailto:agnieszka.jazwa@uj.edu.pl)



hand, such an approach may result in compromised specificity toward cardiomyocytes when compared with cardiac-specific promoter alone.<sup>12</sup> Generation of synthetic promoters combined with cardiomyocyte-specific transcriptional *cis*-regulatory motifs allows for significant improvement of transgene expression in the heart, but a strong off-target effect was visible in the skeletal muscles.<sup>13</sup>

As an alternative to the above-mentioned approaches of targeting transgene expression with cell-specific promoters, negative regulation exploiting tissue specifically expressed miRNAs can be utilized. Incorporation of target sites (TSs) for chosen miRNA into the 3' untranslated region (3' UTR) of the expression cassette enables posttranscriptional regulation of transgene expression in a cell-specific manner.<sup>14</sup> Thanks to RNA interference machinery, if a given miRNA is present in the cells, vectors carrying corresponding TSs are silenced due to degradation of the transgene mRNA or inhibition of translation process.<sup>15</sup> Such strategy was successfully applied for redirecting the tropism of oncolytic viruses<sup>16</sup> and numerous other studies, including cell lineage tracking,<sup>17</sup> detargeting of transgene expression from antigen-presenting cells,<sup>18</sup> or restricting the expression to specific cell types, e.g., interneurons.<sup>19</sup> In case of cardiac muscle, utilization of three tandem repeats of TSs for miRNA-122 (highly expressed in the liver) and genetically engineered TSs for miRNA-206 (referred to as muscle-specific miRNA) in AAV9 vector resulted in efficient transgene delivery to the heart with concomitant repression of its expression in liver and skeletal muscles.<sup>20</sup> In that study, male mice of the BALB/c strain were used, and neither miRNA-122 nor miRNA-206 was expressed in the hearts of these animals.<sup>20</sup>

Here, we aimed to utilize similar, miRNA-122 TS- and mutated miRNA-206 TS-containing self-complementary AAV9 vector (scAAV9-HO1-TS) for cardiac-specific expression of heme oxygenase-1 (HO-1; *HMOX1*) gene. We and others have shown that this stress-inducible enzyme involved in heme catabolism exerts important cardioprotective effects after ischemic injury.<sup>21–23</sup> First, the functionality of scAAV9-HO1-TS vector was confirmed *in vitro*. However, after its systemic administration to the animals lacking HO-1 (HO-1 knockout [KO]; C57BL/6J × FVB strain), there was almost complete repression of transgene expression not only in the liver and skeletal muscles but also in the heart. We found that this was related to the presence of miRNA-122 in the hearts of these animals. What is more, we detected this miRNA not only in the hearts of other commonly used mouse strains but also of patients suffering from various cardiomyopathies and in human cardiomyocytes derived from induced pluripotent stem cells (iPSCs). Importantly, transduction of human iPSC-derived cardiomyocytes with miRNA-122-regulated AAV, similarly to animal studies, resulted in considerable reduction of transgene expression.

## RESULTS

### Assessment of Transgene Expression from the miRNA-122- and miRNA-206-Regulated Vectors

In order to construct scAAV9 vectors for heart-specific overexpression of a chosen transgene, we have cloned human HO-1 coding

sequence under the control of the CMV promoter into the previously generated plasmid backbone containing three tandem repeats of TSs for miRNA-122 and genetically engineered TSs for miRNA-206.<sup>20</sup> miRNA-122 was previously described in several studies as liver specific,<sup>24,25</sup> whereas utilization of the genetically engineered TSs for the muscle-specific miRNA-206 was shown to abrogate its cross-reactivity with miRNA-1 abundant in the heart.<sup>20</sup> Thus, in our study, we have used two miRNA-122- and miRNA-206-controlled constructs: pdAAV-HO1-TS and control pdAAV-HO1-iTS with non-functional, inverted miRNA TS (iTS) region for generation of the scAAV9 vectors (scAAV9-HO1-TS and scAAV9-HO1-iTS, respectively).

First, we evaluated the functionality of scAAV9 harboring the HO1-TS or HO1-iTS expression cassette in HEK293 cells, which are not only highly susceptible to AAV transduction but also do not express any of the regulatory miRNAs (Figure 1A). As a positive control, we used HO-1-carrying vector (scAAV9-HO1) devoid of any miRNA TSs (Figures 1B and 1C). To facilitate transgene detection, we transferred HEK293 cells for 24 h to hypoxic conditions (0.5% O<sub>2</sub>), because in human cells in hypoxia, endogenous HO-1 is downregulated by the Bach-1 repressor.<sup>26</sup> Under hypoxic conditions, transgene overexpression from both vectors was clearly visible and comparable with control scAAV9-HO1 vector (Figures 1B and 1C), confirming the functionality of prepared constructs. In the next step, the vectors were tested in various murine cell lines corresponding to the tissues described as most efficiently transduced by systemically delivered AAV9.<sup>6</sup> We have chosen the AML-12 hepatocyte cell line expressing miRNA-122, C2C12 myoblasts that acquire expression of miRNA-206 as they differentiate to myotubes, and the HL-1 cardiomyocyte cell line characterized by lack of both of those miRNAs (Figure 1A). Because some of the cell lines (HL-1, AML12, and undifferentiated C2C12) turned out to be refractory to AAV9 transduction, they were subjected to transfection only with the corresponding plasmid. We observed considerably lower transgene expression in AML-12 cells transfected with pdAAV-HO1-TS, in comparison with the pdAAV-HO1-iTS with a non-functional regulatory region (Figure 1D). This effect was even more pronounced in differentiated C2C12 cells, where HO-1 expression from the scAAV9-HO1-TS vector was almost completely inhibited (Figure 1E). In contrast, in undifferentiated C2C12 myoblasts, in which the miRNA-206 was barely detectable (Figure 1A), the level of HO-1 protein did not significantly differ between miRNA-regulated pdAAV-HO1-TS and control pdAAV-HO1-iTS plasmid transfection (Figure 1F). Finally, we confirmed the functionality of the HO1-TS expression cassette in the transfected HL-1 cardiomyocyte cell line (Figure 1G) lacking both regulatory miRNAs (Figure 1A) and proceeded with the assessment of *in vivo* cardiac specificity of constructed vectors.

### Analysis of *In Vivo* Functionality of the scAAV9-HO1-TS Vector

The *in vitro* experiments demonstrated that AAV9 harboring miRNA-122 TSs and genetically engineered miRNA-206 TSs may provide heart-specific transduction. Thus, next, we systemically administered scAAV9-HO1-TS and scAAV9-HO1-iTS

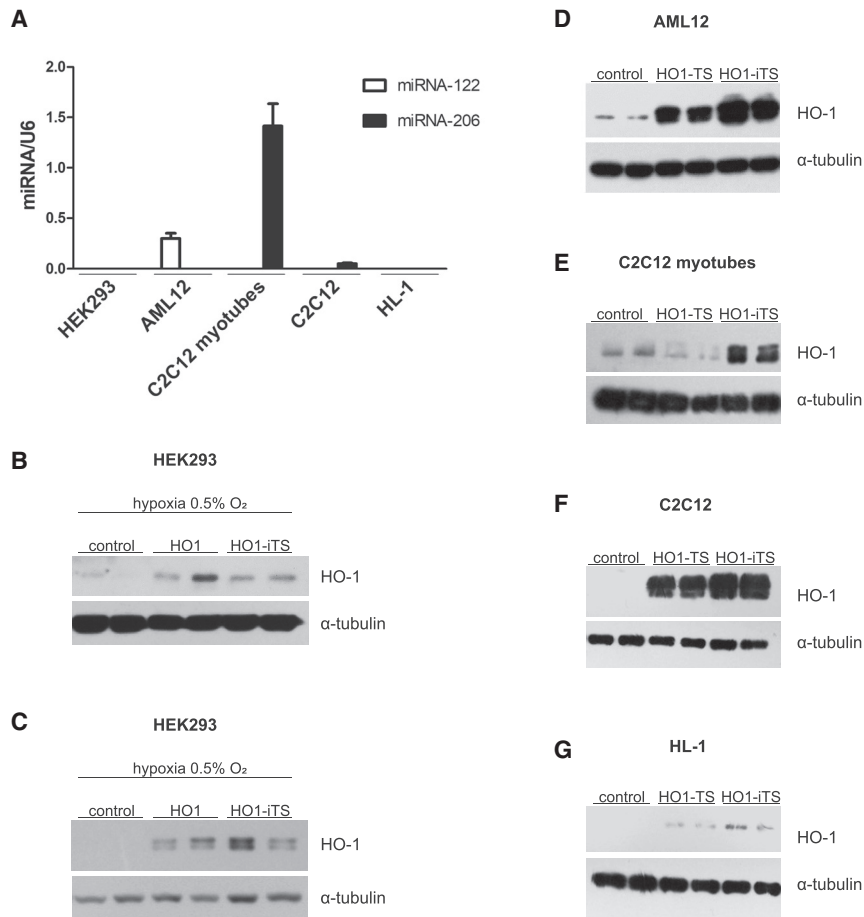


**Figure 1. Transgene Expression from the miRNA-122- and miRNA-206-Regulated Vectors Is Inhibited in Cell Lines Expressing the Corresponding miRNAs**

(A) qPCR analysis of relative miRNA-122 expression in different cell lines, normalized to U6 snRNA. Bars represent mean  $\pm$  SEM (n = 3-5). Representative western blot analysis of HO-1 protein level in: (B) HEK293 cells 7 days after transduction with scAAV9-HO1 (positive control) or scAAV9-HO1-iTS, and hypoxic conditions (0.5% O<sub>2</sub>) were applied 24 h before protein isolation; (C) HEK293 cells 7 days after transduction with scAAV9-HO1 (positive control) or scAAV9-HO1-iTS, and hypoxic conditions (0.5% O<sub>2</sub>) were applied 24 h before protein isolation; (D) AML12 cells 72 h after transfection with pdAAV-HO-TS or pdAAV-HO1-iTS plasmid; (E) differentiated C2C12 cells 7 days after transduction with scAAV9-HO-TS or scAAV9-HO1-iTS vectors; (F) undifferentiated C2C12 cells 72 h after transfection with pdAAV-HO-TS or pdAAV-HO1-iTS plasmid; and (G) HL-1 cells 72 h after transfection with pdAAV-HO-TS or pdAAV-HO1-iTS plasmid. All experiments were performed in duplicate and were repeated at least three times. In all western blot analyses,  $\alpha$ -tubulin served as a loading control.

left panel, white bar). Still, its expression was much lower than in the liver (Figure 2D, right panel, white bar).

Because sex differences may exist in miRNA profiles,<sup>27</sup> we assessed the level of miRNA-122 also in the hearts of male mice of the C57BL/6J  $\times$  FVB strain. It was considerably lower than in female mice (Figure 2D, left panel, black

bar) and again much lower than in liver (Figure 2D, right panel, black bar), but still detectable. Of note, miRNA-122 expression in the heart was not dependent on HO-1, because the same results were obtained in wild-type animals (data not shown). In addition, we checked miRNA-206 expression because its presence in the heart may also cause the same off-target silencing; however, the level of this miRNA was below the detection limit (data not shown).

vectors to 3-month-old HO-1 KO female mice of the C57BL/6J  $\times$  FVB strain. Then, after 4 weeks, the number of vector genome copies, transgene mRNA, and protein level in the heart, liver, and skeletal muscles were assessed. Genome copies (Figure 2A), as well as the HO-1 transcript (Figure 2B) and protein (Figure 2C), were detected in murine hearts and livers following scAAV9-HO1-iTS administration. In skeletal muscles, the background signal (untreated mice) was very high, and thus prevented the estimation of the number of AAV genome copies (Figure 2A); however, transcript and HO-1 protein were successfully detected (Figures 2B and 2C, respectively). What is more, in agreement with previously published data,<sup>20</sup> transgene expression from scAAV9-HO1-TS was completely repressed in the liver and skeletal muscles (Figure 2C), while AAV genomes and transgene mRNA (Figures 2A and 2B, respectively) were detected in those tissues, confirming successful transduction. Surprisingly, we observed a similar effect of scAAV9-HO1-TS in the heart, where despite the presence of AAV genomes (Figure 2A), no HO-1 protein was produced (Figure 2C). Thus, in order to explain this observation, we analyzed the expression of miRNA-122 in the hearts of these animals and found that miRNA-122, described so far as liver specific, is also expressed in the hearts of female C57BL/6J  $\times$  FVB mice (Figure 2D,

bar) and again much lower than in liver (Figure 2D, right panel, black bar), but still detectable. Of note, miRNA-122 expression in the heart was not dependent on HO-1, because the same results were obtained in wild-type animals (data not shown). In addition, we checked miRNA-206 expression because its presence in the heart may also cause the same off-target silencing; however, the level of this miRNA was below the detection limit (data not shown).

Next, we wanted to verify whether a lower expression of miRNA-122 in the hearts of male C57BL/6J  $\times$  FVB mice (Figure 2D) will result in a similar inhibition of transgene expression from the miRNA-controlled vector as in female mice. For this reason, we systemically administered scAAV9-HO1-TS and scAAV9-HO1-iTS vectors to 3-month-old HO-1 KO male mice of the C57BL/6J  $\times$  FVB strain. We confirmed the presence of AAV genomes in hearts and livers (Figure 2E) and the presence of transgene mRNA (Figure 2F) in all analyzed tissues after delivery of both vectors. Moreover, even though in the hearts of male mice HO-1 protein was detectable after administration of scAAV9-HO1-TS vectors, we have noted a very potent (more than 10-fold) repression of transgene expression in comparison with the control scAAV9-HO1-iTS vector (Figure 2G).

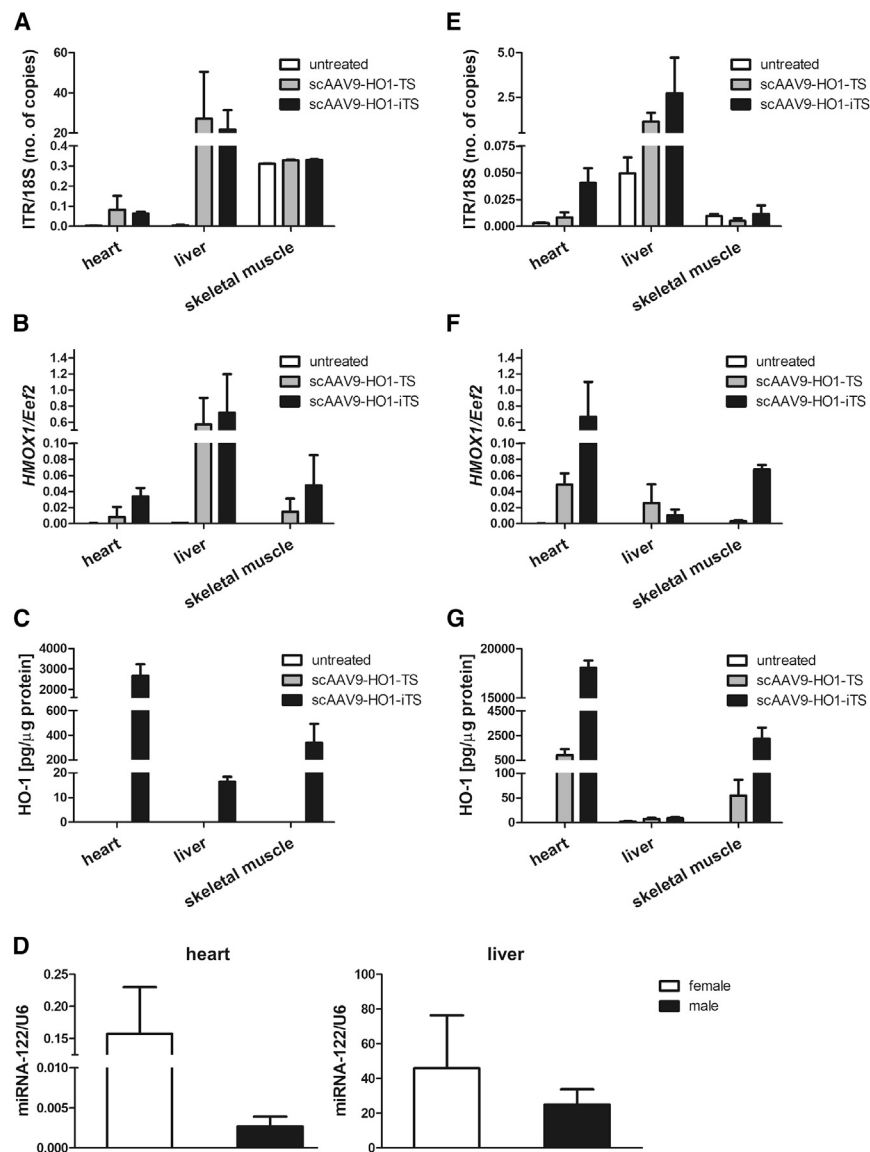


**Figure 2. Transgene Expression from the miRNA-122- and miRNA-206-Regulated Vectors Is Inhibited in Tissues Expressing the Corresponding miRNAs**

(A–G) Female mice of C57BL/6J × FVB strain 4 weeks after intravenous scAAV9 vectors administration ( $n = 3$  mice/group): (A) qPCR quantification of scAAV genomes based on copies of ITR region detected with qPCR using TaqMan probe, normalized to 18S gene copies; (B) qPCR analysis of human HO-1 (*HMOX1*) transcript level; (C) ELISA for human HO-1 protein; (D) qPCR analysis of relative miRNA-122 expression in hearts and livers of female and male mice of C57BL/6J × FVB strain, normalized to U6 snRNA level. Male mice of C57BL/6J × FVB strain 4 weeks after intravenous scAAV9 vectors administration ( $n = 3$  mice/group): (E) qPCR quantification of scAAV genomes based on copies of ITR region detected with qPCR using TaqMan probe, normalized to 18S gene copies; (F) qPCR analysis of human HO-1 (*HMOX1*) gene transcript level; and (G) ELISA for human HO-1 protein. Bars represent mean  $\pm$  SEM in all graphs.

122 also in the hearts of male C57BL/6J, CBA, and DBA mouse strains, as well as in outbred animals (Figure 3B). Thus, strain-related variability of miRNA-122 level in mice was considerable.

Next, we wanted to assess whether the data from murine hearts could reflect the individual differences in humans. For this purpose, we used heart tissue of patients suffering from various cardiomyopathies that was collected during cardiac transplantation. It turned out that miRNA-122 was detectable in all but one heart tissue, and its level differed between patients (Figure 3C).

We also aimed to investigate the potential regulatory mechanisms underlying such considerable variability in miRNA-122 level in the heart.

### Profiling of miRNA-122 Expression in the Hearts of Various Mouse Strains and Patients Suffering from Cardiomyopathies

Previous studies utilized the miRNA-122-controlled vectors in different mouse strains than ours: male BALB/c,<sup>20</sup> male ICR,<sup>28</sup> or NMRI (information about sex was not provided).<sup>29</sup> Thus, we decided to investigate the miRNA-122 expression in the hearts of the mouse strains most widely used in the animal experimentation, namely, C57BL/6J, FVB, CBA, DBA, and BALB/c. In all cases, we used 3-month-old animals. miRNA-122 was clearly detected in both female and male mice of the FVB strain (Figure 3A), with significantly higher expression in females, similarly to our crossbred C57BL/6J × FVB mice (Figure 2D). In male BALB/c mice, miRNA-122 level was low but comparable with the level detected in male C57BL/6J × FVB mice (Figure 3B). Apart from that, we were able to detect miRNA-

We focused on the description in the literature of the main transcriptional regulators of this miRNA expression in the liver, including hepatocyte nuclear factor (HNF) 1-alpha (*HNF1 $\alpha$* ), HNF 3-alpha (*HNF3 $\alpha$* ), HNF 3-beta (*HNF3 $\beta$* ), HNF 4-alpha (*HNF4 $\alpha$* ), and retinoic X receptor-alpha (*RXR $\alpha$* ; *RXRA*).<sup>30,31</sup> Interestingly, the transcripts encoding all of these factors were present in the hearts of FVB, C57BL/6J, C57BL/6J × FVB, and BALB/c mice; however, the expression was uniform among investigated strains (data not shown). In the clinical samples, we detected greater variability in cardiac expression of *HNF1 $\alpha$*  (Figure 3D), *HNF3 $\beta$*  (Figure 3E), and *RXRA* (Figure 3F). Interestingly, the profile of *RXRA* expression (Figure 3F) to some extent corresponded with miRNA-122 (Figure 3C), suggesting a possible regulatory mechanism of this miRNA expression in the human heart.



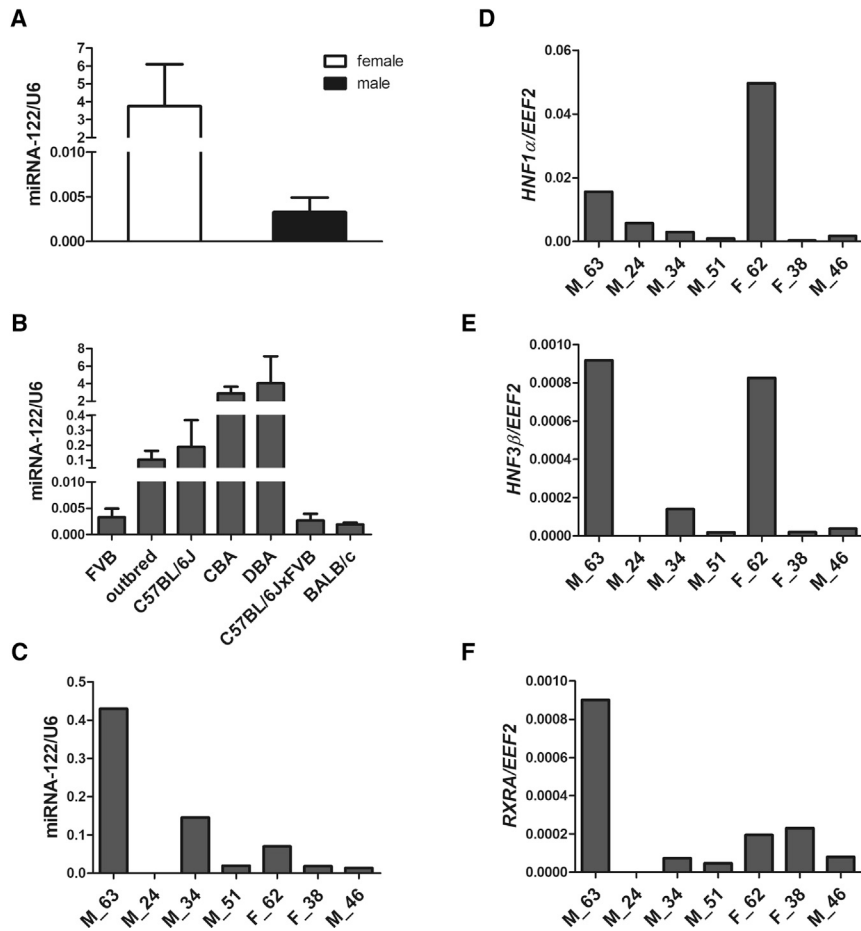


**Figure 3. Cardiac miRNA-122 Expression Varies between Various Mouse Strains and between Human Individuals**

(A–C) qPCR analysis of miRNA-122 expression in (A) hearts of female and male mice of FVB strain ( $n = 5$  mice/group), (B) hearts of male mice of various strains ( $n = 5$  of FVB, outbred, C57BL/6J, DBA, C57BL/6J  $\times$  FVB, BALB/c mice/group;  $n = 3$  of CBA mice/group), and (C) heart tissues collected from patients suffering from different cardiomyopathies. (D–F) qPCR analysis of (D) *HNF1 $\alpha$* , (E) *HNF3 $\beta$* , and (F) *RXRA* expression in heart tissues collected from patients suffering from different cardiomyopathies. Bars represent mean  $\pm$  SEM in all graphs. Sample description: F, female; M, male; number, age of the patient undergoing heart transplantation.

of GFP<sup>+</sup> cells (Figure 4B) and median fluorescence intensity (MFI) (Figure 4C) following scAAV9-GFP-TS were approximately by half smaller than after control scAAV9-GFP-iTS vector transduction.

## DISCUSSION

Despite numerous successful applications of gene therapy developed in recent years, many aspects regarding the design of safe and effective vectors remain challenging. One of these concerns is specific transgene delivery to the chosen tissues. Although wide tropism of some AAV vectors facilitated their potential application in the treatment of many diseases, it may be considered also as one of their shortcomings.

Off-target transduction might not only disrupt the homeostasis of cells unaffected by a given disease but also contribute to the development of immune response against delivered transgene (reviewed in Boisgerault and Mingozzi<sup>35</sup>). Such an effect was already observed in some studies involving *in vivo* AAV-mediated transgene introduction. Although expression of the transgene in the liver is mostly associated with tolerogenic response,<sup>36</sup> in the skeletal muscles it is likely to induce transgene-specific CD8<sup>+</sup> T cell infiltration into the tissue.<sup>37,38</sup>

In case of cardiac muscle, very efficient gene delivery can be achieved using AAV serotype 9; however, transduction will occur also in the liver and skeletal muscles.<sup>3</sup> To restrict transgene expression only to the heart, the expression cassette may contain regulatory sequences responding to endogenously expressed miRNAs. Previous studies have shown that incorporation of tandem repeats of liver-specific miRNA-122 TSs and skeletal muscle-specific miRNA-206 genetically modified TSs into the 3' UTR of expression cassette allows for post-transcriptional de-targeting of transgene expression from these tissues, and thus for the generation of heart-specific AAV9 vectors.<sup>20,28,29</sup> In our study, we have confirmed the functionality of the HO1-TS and HO1-iTS expression cassettes in various cell lines, showing that the expression of the transgene is indeed dependent

## Analysis of miRNA-Regulated Vector Functionality in Human Cardiomyocytes

Finally, we aimed to analyze whether transgene expression in human cardiomyocytes may be subjected to, similar as in animal studies, miRNA-122-mediated posttranscriptional regulation. Due to a well-known difficulty in obtaining primary human cardiomyocytes and their very limited proliferation potential,<sup>32,33</sup> for this purpose we utilized human iPSC-derived cardiomyocytes. First of all, we detected miRNA-122 in the cells from all three healthy donors (Figure 4A). Next, these iPSC-derived cardiomyocytes were transduced with scAAV9-GFP-TS and scAAV9-GFP-iTS. Here, the HO-1 harboring vectors were replaced with GFP-expressing ones to avoid a possible influence of endogenous HO-1 expression and its variability between different donors on the final outcome. Additionally, because cardiomyocytes were derived from different donors, we wanted to minimize the effect of potential variations in AAV9 receptor availability on the transduction efficiency. Thus, before transduction, cardiomyocytes were treated with neuraminidase to expose N-linked galactose on the surface of the cells, which is the primary receptor for AAV9.<sup>34</sup> The level of miRNA-122 was relatively low in all three lines of human iPSC-derived cardiomyocytes (Figure 4A), but it was still sufficient to effectively inhibit transgene expression, because both the percentage

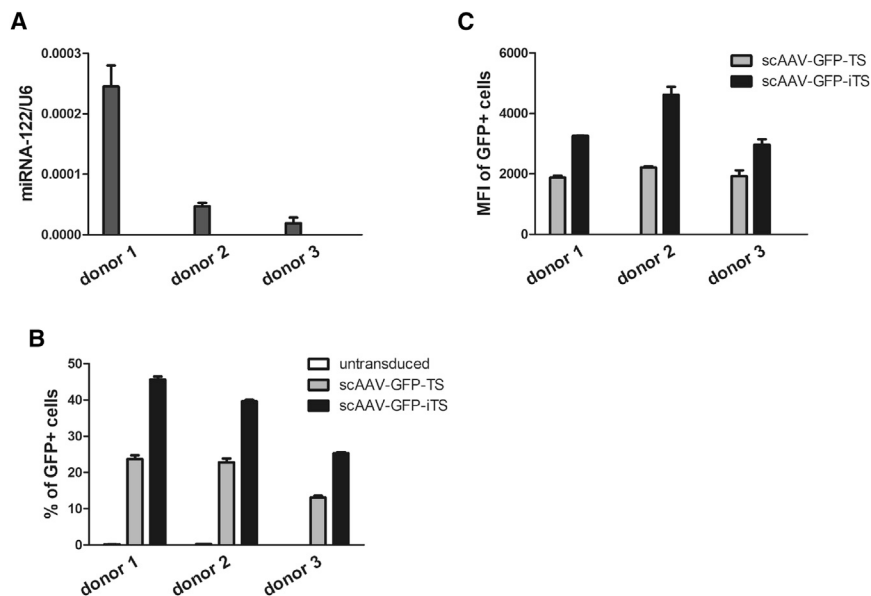


**Figure 4. Transgene Expression from the miRNA-122- and miRNA-206-Regulated Vectors Is Inhibited in Human iPSC-Derived Cardiomyocytes**

(A) qPCR analysis of relative miRNA-122 expression in human iPSC-derived cardiomyocytes from three different iPSC donors. (B and C) Flow cytometric analysis of (B) percentage of GFP-expressing cells and (C) median fluorescence intensity (MFI) 96 h after transduction of human iPSC-derived cardiomyocytes with scAAV9-GFP-TS or scAAV9-GFP-iTS vectors. All experiments were performed in duplicate. Bars represent mean  $\pm$  SD in all graphs.

on the level of miRNA-122 and miRNA-206 in the given cell type. Importantly, the HL-1 cardiomyocyte cell line did not contain any of these miRNAs, and consequently transgene was expressed after transfection with both iTS- and TS-carrying vectors. Surprisingly, when we intravenously administered scAAV9-HO1-TS to HO-1 KO female mice, we did not detect HO-1 protein in the hearts of these animals, despite the presence of scAAV genomes and transgene mRNA in the tissue. This result was in striking contrast with other studies showing that incorporation of the target sequence of miRNA-122 into the 3' UTR of the expression cassette led to heart-specific transgene expression.<sup>28,29,39</sup>

As the major difference between current and previously published data, we have identified the strain of mice (C57BL/6J  $\times$  FVB versus BALB/c, ICR, NMRI or Ai9  $\times$  C57BL/6). We detected considerable expression of miRNA-122 in the hearts of our C57BL/6J  $\times$  FVB female mice, which resulted in complete repression of transgene expression in this tissue following application of scAAV9-HO1-TS vectors. In some of the previous studies, male mice were used; thus, taking into account that sex differences may determine the miRNA profile,<sup>27</sup> we checked the miRNA-122 expression also in male C57BL/6J  $\times$  FVB mice and found that it was significantly lower than in females. This, however, also resulted in substantial, although not complete, repression of transgene expression in the heart following systemic scAAV9-HO1-TS vectors administration. Still, we cannot exclude that other factors apart from miRNA-122, e.g., hormones, may influence the efficiency of transgene expression and partially contribute to the observed discrepancies between male and female mice.

The analysis of miRNA-122 expression in the hearts of male mice of various strains revealed substantial differences. We detected relatively high levels of this miRNA in the hearts of a few commonly used mouse strains, including FVB, C57BL/6J, DBA, and CBA. Moreover,

even though the level of cardiac miRNA-122 in male C57BL/6J  $\times$  FVB and BALB/c mice was comparable and the lowest among all analyzed mouse strains, in contrary to previously published data,<sup>20,29</sup> we observed partial repression of the transgene in the heart. The main factor accounting for that outcome may be very high sensitivity of the regulatory system to any changes in miRNA-122 due to the presence of tandem repeats of the TS region.<sup>40</sup> Furthermore, the sensitivity of the miRNA-driven regulation is also influenced by the surrounding sequences and the proximity of TSs to the STOP codon of the transgene coding sequence,<sup>41</sup> which differ between ours and previous studies. Another factor that may contribute to the observed discrepancies between the studies on miRNA-122-regulated vectors may be the age of the animals used in the experiments. Whereas BALB/c mice utilized previously were around 6 weeks old,<sup>20</sup> here we analyzed 3-month-old animals. Although this difference seems to be quite low, our results suggest that miRNA-122 expression in the heart of some mouse strains may increase with the age of the animal (unpublished data). Apart from that, we should also take into consideration that different sources of mice used in the experiments might introduce additional fluctuations.

Importantly, here we demonstrate that similar variability in cardiac miRNA-122 expression may exist also in humans. Several studies described miRNA-122 as liver specific because of high expression in this organ.<sup>25,42</sup> Interestingly, the plasma level of this miRNA was remarkably upregulated in patients with hyperlipidemia compared with healthy controls, and it was closely associated with the presence and the severity of coronary heart disease (CHD) in hyperlipidemia patients.<sup>43</sup> A recent meta-analysis demonstrated stable changes of miRNA-122-5p in CHD subjects, indicating that it may be a potentially useful therapeutic target.<sup>44</sup> Although miRNA-122 expression is the highest in liver, it was also detected in the nervous and respiratory systems.<sup>25</sup> Here we show that miRNA-122 is present also in the hearts of patients suffering from various cardiomyopathies. In the future, having the opportunity to analyze a larger group of patients, it might be worth it to correlate this miRNA expression profile with age, sex, or particular disease. If a specific disorder could influence miRNA-122 level in the heart, it would also determine the

effectiveness of gene therapy with miRNA-regulated AAV. Although very limited, there is some evidence supporting the role of miRNA-122 in the regulation of cardiomyocyte apoptosis influencing the expression of caspase-8.<sup>45,46</sup> Interestingly, an increase in miRNA-122 in rat cardiomyocytes was induced by hypoxia/reperfusion, demonstrating its potential role in cardiac pathologies.<sup>47</sup>

Transcriptomic and proteomic analyses included in Human Protein Atlas (<https://www.proteinatlas.org/>) provide data supporting the presence of several potential positive regulators of miRNA-122 level in the human heart, including HNF4 $\alpha$  and RXR $\alpha$ . Moreover, according to Expression Atlas (<http://www.ebi.ac.uk/gxa>), Hnf4 $\alpha$  and Rxr $\alpha$  are also expressed in murine heart. Although we confirmed the presence of Hnf1 $\alpha$ , Hnf3 $\alpha$ , Hnf3 $\beta$ , Hnf4 $\alpha$ , and Rxra in the hearts of various mouse strains, there were no significant differences in their expression (data not shown). In contrast, patient samples exhibited more variability, and particularly the expression of RXRA to some extent corresponded with the expression of miRNA-122. Obviously, because these factors were described as miRNA-122 expression regulators in the liver,<sup>30,31</sup> interpretation of our data in the heart is more complex, because different, yet unknown, regulatory pathways can be involved. Still, it is important that HNFs are expressed in cardiac tissue and consequently might influence the expression of co-existing genes or miRNAs. This, however, would require further investigation.

In this study, we also tested human cardiomyocytes obtained from iPSCs in terms of potential miRNA-122-mediated posttranscriptional regulation of transgene expression. Human iPSC-derived cardiomyocytes are used in basic and translational cardiac research to model cardiovascular diseases, study drug toxicity, and advance potential regenerative therapies.<sup>48,49</sup> They are also susceptible to AAV9 transduction. Even though miRNA-122 level was relatively low in human cardiomyocytes derived from all three iPSC cell lines, similar to animal studies, we observed downregulation of transgene expression following transduction with miRNA-122-regulated AAV9 in comparison with control vector with inverted TS region. These data further underline the significance of miRNA-122 expression in the heart and its impact on the final outcome of the therapy utilizing miRNA-regulated vectors. On the other hand, it should also be considered that iPSC-derived cardiomyocytes exhibit rather immature phenotype, when compared with adult cardiomyocytes, and are functionally closer to prenatal cardiomyocytes.<sup>50,51</sup> This feature may contribute to the low miRNA-122 expression in our iPSC-derived cardiomyocytes. Previous study by Kuppusamy et al.<sup>52</sup> demonstrated that miRNA-122 was one of the significantly upregulated miRNAs in conditioned engineered heart tissue when compared with 1-year matured human embryonic stem cell-derived cardiomyocytes, indicating a possible regulation of this miRNA during cardiomyocyte maturation. Thus, in the future, a long-term culture of iPSC-derived cardiomyocytes and other treatments that improve their maturity<sup>52</sup> can be applied to increase the translational potential of these cells. Subsequent investigation and comparison of the miRNA expression profile of such mature cardiomyocytes with pri-

mary human cardiomyocytes could create new opportunities in screening patients for miRNA-regulated therapy.

In summary, our data indicate high sensitivity of the miRNA-regulatory system to any variations in the corresponding endogenous miRNA expression. This underlines the importance of choosing the appropriate animal model for the preclinical evaluation of therapy effectiveness, as in some cases the final results may be heavily influenced by the genetic background. Moreover, inter-individual differences in the human cardiac miRNA-122 expression raise some doubts regarding widespread clinical application of such regulation strategy. Even though there might be a fraction of patients who could potentially benefit from such therapy utilizing miRNA-122-regulated AAV vectors, qualification of patients based on prior non-invasive assessment of the miRNA-122 level in the heart would be necessary.

## MATERIALS AND METHODS

### Animals

BALB/c, DBA, CBA, and outbred mice were acquired from the breeding colony at the Institute of Zoology of Jagiellonian University (Krakow, Poland). C57BL/6J and FVB mice were obtained from a breeding colony at the Mossakowski Medical Research Centre, Polish Academy of Sciences (Warsaw, Poland). *Hmox1*<sup>-/-</sup> C57BL/6J  $\times$  FVB mice (HO-1 KO) were generated at the Faculty of Biochemistry, Biophysics and Biotechnology, Jagiellonian University (Krakow, Poland) from the *Hmox1*<sup>+/-</sup> heterozygous breeding pairs kindly gifted by Dr. Anupam Agarwal (Birmingham, AL, USA). All mice used in the experiments were 3 months old. All animal procedures were conducted in accordance with *Guide for the Care and Use of Laboratory Animals* (Directive 2010/63/EU of European Parliament) and carried out under a license from the Ethical Committee of the Jagiellonian University. Animals were maintained under controlled environmental conditions (12-h light/dark cycle, at approx. 23°C) and provided with standard laboratory food and water *ad libitum*.

### Construction of Plasmids

Plasmids for production of scAAV9 vectors regulated by miRNA-122 and miRNA-206 expression were prepared using Gibson Assembly Master Mix (catalog [cat.] #E2611; NEB, Ipswich, MA, USA) through replacement of S100A coding sequence with the sequence encoding human HO-1 in previously cloned and described plasmids: pscAAV-CMV-MLC0.26-NFS100A1<sub>miR-122(3x)TS/m206(3x)TS-3G</sub> with miRNA-122 TS and mutated miRNA-206 TS or pscAAV-CMV-MLC0.26-NFS100A1<sub>invTS</sub>, where the TS region of both miRNAs has been inverted and thus non-functional.<sup>20</sup> In addition, instead of the hybrid CMV-MLC0.26 promoter, we utilized the CMV promoter. In this manner we have generated, respectively, pdAAV-CMV-HO1-TS (pdAAV-HO1-TS) and pdAAV-CMV-HO1-iTS (pdAAV-HO1-iTS) plasmids for scAAV9 production. Similar constructs were prepared with GFP transgene under the control of a CMV promoter: pdAAV-CMV-GFP-TS (pdAAV-GFP-TS) and pdAAV-CMV-GFP-iTS (pdAAV-GFP-iTS). Primers with specific adapters that enabled assembly were designed using NEBulider Assembly Tool. Schematic representation of plasmid maps was generated with SnapGene Viewer

Software (plasmid map is available in the [Supplemental Information; Figure S1](#)). Following cloning steps, all plasmids were subjected to Sanger sequencing to ensure correct insertion of the transgene.

### Production of AAV Vectors

The scAAV9 vectors were produced in a helper-free, three-plasmid system using CellRoll Bottle Roller (Integra Biosciences, Zizers, Switzerland). For this purpose, AAV293 packaging cells (HEK293 subclone) were seeded on collagen-coated Roller Bottles (cat. #431198; Corning, NY, USA) and cultured until they reached 50%–60% confluence. Next, the cells were transfected with 130  $\mu$ g pHelper (Stratagene, San Diego, CA, USA), 100  $\mu$ g p5E18VD2/9 (kindly provided by Prof. James Wilson, University of Pennsylvania, Philadelphia, PA, USA), and 90  $\mu$ g pdAAV-CMV-HO1 (without any miRNA TS), pdAAV-CMV-HO1-TS, pdAAV-CMV-HO1-iTS, pdAAV-CMV-GFP-TS, or pdAAV-CMV-GFP-iTS plasmids utilizing PEI MAX (cat. #24765; Polysciences, Warrington, PA, USA) as a transfection reagent (2.58 mg/mL; 1  $\mu$ L per 1  $\mu$ g DNA). After 72 h, cells were detached from the culture surface, centrifuged, and lysed through three freeze-thaw cycles in liquid nitrogen and 37°C water bath. Then, lysates were digested with HS nuclease (cat. #GENUC10700-01; MoBiTec, Göttingen, Germany) in a final concentration of 50 U/mL for 1 h at 37°C and subsequently precleared by centrifugation for 30 min at 4,000  $\times$  g, 4°C. Precleared lysates were further purified through ultracentrifugation (300,000  $\times$  g, 2 h, 18°C) on discontinuous iodixanol gradient (gradient composition: 17 mL of processed crude lysate, 6 mL of 15% iodixanol, 4.5 mL of 25% iodixanol, 3.5 mL of 40% iodixanol, and 3.5 mL of 54% iodixanol). Iodixanol dilutions were prepared in PBS with 0.5 mM MgCl<sub>2</sub> and 2.5 mM KCl. After ultracentrifugation, 40% iodixanol fraction containing AAV vectors was collected and was further concentrated on Amicon Ultra-15 Centrifugal Filters (cat. #UFC910024; 100 kDa; Merck Millipore, Burlington, MA, USA).

Next, using phenol-chloroform extraction, we isolated DNA from a small portion of purified vectors to quantify the number of viral genomes (vg). Titration of AAV genome copies was carried out using quantitative PCR (qPCR) with inverted terminal repeat (ITR)-binding TaqMan probe with serial dilutions of linearized plasmid as standard curve. qPCR was prepared using TaqMan Gene Expression Master Mix, according to the manufacturer's instructions with specific primers and TaqMan probe in a final concentration of 100 nM (For [Forward]: 5' CGGCCTCAGTGAGCGA; Rev [Reverse]: 5'-GGAACCCCTAGTGATGGAGTT; Probe: 5'-6-FAM-CACTCCCTCTCTGCGCGCTCG-BHQ-1).

### Cell Culture, Transfection, and Transduction Assays

HEK293 and mouse C2C12 cells (ATCC, Manassas, VA, USA) were cultured in DMEM high-glucose medium supplemented with 10% fetal bovine serum (FBS) and antibiotics (penicillin 100 U/mL, streptomycin 100  $\mu$ g/mL). Differentiation of C2C12 cells to myotubes was carried out for 5 days in the conditions of reduced growth factors availability, where FBS in the culture medium was replaced by 2% horse serum.<sup>53</sup> HL-1 mouse cardiac myocytes (cat. #SCC065;

Sigma-Aldrich, Saint Louis, MO, USA) were cultured in Claycomb medium (cat. #51800C; Sigma-Aldrich) supplemented with 10% FBS, GlutaMAX I CTS (cat. #A1286001; GIBCO), norepinephrine (0.1 mM; cat. #A0937; Sigma-Aldrich), and antibiotics. AML12 mouse hepatocytes (cat. #CRL-2254; ATCC, Manassas, VA, USA) were cultured in DMEM/F12 medium supplemented with 10% FBS and Insulin -Transferrin-Selenium (ITS supplement; ATCC): insulin (0.005 mg/mL), transferrin (0.005 mg/mL), selenium (5 ng/mL), and with dexamethasone (40 ng/mL) in the presence of antibiotics. All cells were maintained under standard culture conditions (37°C, 5% CO<sub>2</sub>, humidified atmosphere).

For the assessment of the functionality of prepared constructs, cells were transfected with either PEI MAX (HEK293) or Lipofectamine 2000 (C2C12, HL-1, AML12) and transgene-encoding plasmid. The functionality of scAAV vectors was tested through transduction of target cells with multiplicity of infection (MOI) of 10,000 vg/cell. Transgene expression was monitored up to 7 days after transduction.

### In Vivo Administration of AAV Vectors

AAV vectors (scAAV9-HO1-TS and scAAV9-HO1-iTS) were administered systemically through tail vein injection to 3-month-old male and female HO-1 KO mice of C57BL/6J  $\times$  FVB strain at the dose of 5  $\times$  10<sup>11</sup> vg/animal. After 4 weeks, mice were euthanized with CO<sub>2</sub> and immediately perfused through the left ventricle with PBS containing 0.5 U/mL heparin. Hearts, livers, and gastrocnemius muscles were collected, snap frozen in liquid nitrogen, and stored at –80°C for further analysis.

### Western Blotting

Cells were washed twice with ice-cold PBS and scratched from the plate in 1% Triton X-100 in PBS with addition of EDTA-free cComplete Protease Inhibitor Cocktail (cat. #11873580001; Roche, Basel, Switzerland). After centrifugation (10,000  $\times$  g, 10 min, 4°C), supernatants were collected and protein concentration was determined using DC Protein Assay (cat #5000112; Bio-Rad, Hercules, CA, USA) according to the manufacturer's instructions.

Samples prepared in reducing, denaturing conditions (15–30  $\mu$ g of protein) were loaded on 12% gel followed by SDS-PAGE electrophoresis (150 V through the stacking gel, 200 V through the separating gel). Then, wet transfer to 0.45  $\mu$ m nitrocellulose membrane was performed (100 V, 1 h). Next, membranes were incubated in blocking buffer (5% nonfat dry milk in Tris-buffered saline [TBS]) for 1 h at room temperature (RT) and transferred to solutions of primary antibodies ( $\alpha$ -tubulin antibody, clone: B-5-1-2 [Sigma-Aldrich], cat. #T5168; HO-1 antibody, polyclonal [Enzo, Farmingdale, NY, USA], cat. #ADI-SPA-894-F) diluted 1,000 times in blocking buffer. Following overnight incubation at 4°C, membranes were washed five times with TBS containing 0.1% Tween 20, and subsequently secondary antibodies conjugated with horseradish peroxidase diluted in blocking buffer were added for 1 h at RT. After repeating the washing steps, chemiluminescent substrate was added for 5 min, and membranes were manually developed.



**Table 1. Characteristics of the Patients**

Patient ID	Sex	Age (Years)	Disease
M_63	male	63	ischemic cardiomyopathy
M_24	male	24	cardiomyopathy
M_34	male	34	restrictive cardiomyopathy
M_51	male	51	dilated cardiomyopathy
F_62	female	62	congestive heart failure
F_38	female	38	cardiomyopathy, heart failure
M_46	male	46	chronic heart failure

### Assessment of AAV Genome Copies in Tissues

In the first step, tissue fragments were homogenized in protein digestion buffer (10 mM EDTA, 1% SDS, and 400 µg/mL Proteinase K in 500 µL TBS) and incubated for 1 h at 37°C. Next, equal volume of phenol-chloroform-isoamyl alcohol (25:24:1, cat. #P3803; Sigma-Aldrich) was added, and samples were vortexed vigorously for 1 min. To allow separation of phases, samples were centrifuged (12,000 × g, 15 min, RT), and then the top, aqueous phase was transferred to new tubes and subsequently mixed with 1 mL absolute ethanol and 10 µL of 5 M NaCl. Next, in order to enable DNA precipitation, the samples were incubated overnight in −20°C. The following day, after centrifugation (12,000 × g, 15 min, RT) and washing of DNA with 70% ethanol, samples were air-dried and resuspended in nuclease-free water. The number of AAV genome copies in tissues was assessed utilizing qPCR method with TaqMan probe as described in the AAV titration procedure above and normalized to 18S rRNA expression.

### RNA Isolation, Reverse Transcription, and qPCR

Total RNA was isolated by lysing the samples in TRIzol reagent (cat. #15596026; Thermo Fisher Scientific, Waltham, MA, USA) followed by phenol-chloroform extraction and isopropanol precipitation. For analysis of gene expression, synthesis of cDNA was conducted with RevertAid reverse transcriptase (cat. #EP0441; Thermo Fisher Scientific) according to manufacturer's instructions using 1 µg RNA. qPCR was performed using StepOne Plus Real-Time PCR (Applied Biosystems, Foster City, CA, USA) with reaction mix composed of SYBR Green PCR Master Mix (SYBR Green JumpStart *Taq*, cat. #S4438; Sigma-Aldrich), 20 ng of a template, and transgene-specific primers (final concentration 500 nM; Table 1). Elongation factor 2 (*EEF2*, *Eef2*) served as a housekeeping gene in all mRNA expression analyses. Primer sequences were as follows: *EF2* For: 5'-TCAGCAC ACTGGCATAGAGG-3', Rev: 5'-GACATCACCAAGGGTGTGCA-3'; *HMOX1* (*HO-1*) For: 5'-GGAGGTCATCCCCTACACAC-3', Rev: 5'-CTGGGAGCGGGTGTGAGTG-3'; *HNF1a* For: 5'-ACA GCTTGGAGCAGACATCC-3', Rev: 5'-CTGCTTGGTGGCGGTG AG-3'; *HNF3b* (*FOXA2*) For: 5'-AATCTCAGCCTCCAACCGTC-3', Rev: 5'-CGGCGTTCATGTTGCTCAC-3'; *RXRα* For: 5'-CATTTCCTGCCGCTCGATTT-3', Rev: 5'-GCTGACGGGGTTCATAGG TG-3'; *18S rRNA* For: 5'-CCAGAGCGAAAGCATTTGCCAAGA-3', Rev: 5'-GCATTGCCAGTCGGCATCGTTTAT-3'.

In case of miRNA expression analysis, miRCURY LNA RT Kit (cat. #339340; QIAGEN, Hilden, Germany) was utilized for reverse transcription together with compatible miRCURY LNA miRNA PCR Assay (cat. #339345; QIAGEN) and predesigned locked nucleic acid (LNA) primers (QIAGEN) recognizing miRNA-122-5p (cat. #MS00003416), miRNA-206-5p (cat. #MS00003787), and U6 small nuclear RNA (snRNA; cat. #MS00033740); the last one was used for normalization of the results. Analysis of melt curves, in order to ensure specificity of the products, was conducted using StepOne Software v.2.3.

### ELISA

Fragments of tissues (heart, liver, and skeletal muscle) were homogenized in 1% Triton X-100 in PBS with addition of EDTA-free cOmplete Protease Inhibitor Cocktail using TissueLyser homogenizer (QIAGEN). Protein concentration was determined using DC Protein Assay according to the manufacturer's instructions. Human HO-1 level was assessed using Simple Step ELISA (cat. #ab207621; Abcam, Cambridge, UK) in samples diluted to match the assay's dynamic range, according to the manufacturer's instructions.

### Patient Samples

Heart tissue was obtained from the left ventricle of seven patients suffering from various cardiomyopathies who were undergoing heart transplantation surgery, under approval of the Institutional Review Board and Bioethical Committee and with informed consent, in accordance with the Declaration of Helsinki. The characteristics of patients from whom the material was collected and used in this study are provided in Table 1. Tissue fragments were stored for 24 h in RNAlater solution (cat. #AM7020; Thermo Fisher Scientific) at 4°C and then transferred to −80°C for further storage.

### Differentiation of Human iPSC-Derived Cardiomyocytes

Peripheral blood mononuclear cells (PBMCs) were isolated from three healthy volunteers under approval of the Institutional Review Board and Bioethical Committee and with informed consent, in accordance with the Declaration of Helsinki. The characteristics of these donors are provided in Table 2.

PBMCs were reprogrammed to iPSCs with use of non-integrating Sendai vectors (Cytotune-iPS 2.0 Sendai Reprogramming kit, cat. #A16517; Thermo Fisher Scientific) according to the manufacturer's protocol. The pluripotency of all generated human iPSC lines was confirmed (data not shown) as described by us previously<sup>54</sup> prior to using the cells in further experiments.

Human iPSCs were cultured on Geltrex-coated 12-well plates (Geltrex LDEV-Free hESC-Qualified Reduced Growth Factor Basement Membrane Matrix, cat. #A1413302; Thermo Fisher Scientific) in Essential 8 medium (cat. #A1517001; Thermo Fisher Scientific) and passaged using 0.5 mM EDTA. The ROCK inhibitor Y-27632 (cat. #ab120129; 10 µM; Abcam) was added to the culture medium for the first 24 h after passage. Differentiation toward cardiomyocytes was performed according to the protocol published by Lian et al.<sup>55</sup>

**Table 2. Characteristics of the iPSC Donors**

ID	Sex	Age (Years)
Donor 1	male	55
Donor 2	male	48
Donor 3	male	70

Particularly, CHIR99021 (cat. #SML1046-5MG; 8–12  $\mu$ M optimized independently for each cell line; Sigma-Aldrich) and IWR-1 (cat. #I0161-5MG; 5–7  $\mu$ M; Sigma-Aldrich) were used as small molecules regulating the WNT pathway. Cells were subjected to metabolic selection from days 10 to 16 by culture in medium consisting of RPMI 1640 without glucose supplemented with 2% B-27 supplement (cat. #17504044; Thermo Fisher Scientific) and 4 mM sodium DL-lactate (cat. #L1375-500ML; Sigma-Aldrich), followed by passage and further culture until days 20–30 in RPMI 1640 containing 2% B27 supplement. All cells were maintained in a humidified tissue culture incubator at 37°C and 5% CO<sub>2</sub>.

#### Phenotyping of Human iPSC-Derived Cardiomyocytes

Differentiated human iPSC-derived cardiomyocytes were detached from a culture surface with use of TrypLE Select Enzyme (cat. #A1217701; Thermo Fisher Scientific) to obtain single-cell suspension. After washing with PBS containing 2% FBS, cells were fixed and permeabilized using BD IntraSure Kit (cat. #641778; Becton Dickinson, NJ, USA), followed by 45-min incubation with primary antibodies recognizing cTnT (Cardiac Troponin T Monoclonal Antibody, 1:1,000, clone 13-11; cat. #MA512960; Thermo Fisher Scientific). Subsequently, the antibodies were washed out, and the cells were incubated for 20 min with secondary antibodies conjugated with Alexa Fluor 488 [Rabbit anti-Mouse IgG (H+L), Superclonal Recombinant Secondary Antibody, 1:500; cat. #A27023; Thermo Fisher Scientific]. Nuclei were counterstained with 0.2  $\mu$ g/mL DAPI (cat. #D9542; Sigma-Aldrich).

All iPSC lines displayed successful cardiomyocyte differentiation with spontaneous beating and between 55% and 89.6% cTnT<sup>+</sup> cells (Figure S2) as determined by flow cytometric analysis using LSRFortessa flow cytometry analyzer (BD Biosciences) and BD FACSDiva Software.

#### Transduction of Human iPSC-Derived Cardiomyocytes

Differentiated human iPSC-derived cardiomyocytes were treated with neuraminidase type III (50 mU/mL, cat. #11080725001; Sigma-Aldrich) for 2 h to expose AAV9 receptor (N-linked galactose)<sup>34</sup> on the surface of the cells and were subsequently transduced with MOI = 10<sup>4</sup> vg/cell of either scAAV9-GFP-TS or scAAV9-GFP-iTS vector. After 96 h, the number of GFP<sup>+</sup> cells and MFI were analyzed using LSRFortessa flow cytometry analyzer (BD Biosciences) with BD FACSDiva Software.

#### SUPPLEMENTAL INFORMATION

Supplemental Information can be found online at <https://doi.org/10.1016/j.omtm.2020.05.006>.

#### AUTHOR CONTRIBUTIONS

I.K. and M.T. conceived and performed experiments. K.A. and J.S. generated and provided the human iPSC-derived cardiomyocytes. M.B., A.G., H.F., and J.D. provided reagents and expertise. J.D. secured funding. M.Z. provided patient samples and expertise. A.J.-K. designed experiments and secured funding. I.K. took the lead in writing the manuscript. All authors provided critical feedback and helped to shape the research, analysis, and manuscript.

#### CONFLICTS OF INTEREST

The authors declare no competing interests.

#### ACKNOWLEDGMENTS

This work was supported by SONATA BIS grant 2014/14/E/NZ1/00139 (to A.J.-K.) and HARMONIA grant 2014/14/M/NZ1/00010 (to J.D.), both from the National Science Centre. The graphical abstract was partially designed using Servier Medical Art according to a Creative Commons Attribution 3.0 Unported License guidelines 3.0 (<http://creativecommons.org/licenses/by/3.0/pl/>).

#### REFERENCES

- Wang, D., Tai, P.W.L., and Gao, G. (2019). Adeno-associated virus vector as a platform for gene therapy delivery. *Nat. Rev. Drug Discov.* 18, 358–378.
- Naso, M.F., Tomkowicz, B., Perry, W.L., 3rd, and Strohl, W.R. (2017). Adeno-Associated Virus (AAV) as a Vector for Gene Therapy. *BioDrugs* 31, 317–334.
- Zincarelli, C., Soltys, S., Rengo, G., and Rabinowitz, J.E. (2008). Analysis of AAV serotypes 1–9 mediated gene expression and tropism in mice after systemic injection. *Mol. Ther.* 16, 1073–1080.
- Büning, H., and Srivastava, A. (2019). Capsid Modifications for Targeting and Improving the Efficacy of AAV Vectors. *Mol. Ther. Methods Clin. Dev.* 12, 248–265.
- Hartikainen, J., Hassinen, I., Hedman, A., Kivela, A., Saraste, A., Knuuti, J., Husso, M., Mussalo, H., Hedman, M., Rissanen, T.T., et al. (2017). Adenoviral intramyocardial VEGF- $\Delta$ N $\Delta$ C gene transfer increases myocardial perfusion reserve in refractory angina patients: a phase I/IIa study with 1-year follow-up. *Eur. Heart J.* 38, 2547–2555.
- Inagaki, K., Fuess, S., Storm, T.A., Gibson, G.A., Mctiernan, C.F., Kay, M.A., and Nakai, H. (2006). Robust systemic transduction with AAV9 vectors in mice: efficient global cardiac gene transfer superior to that of AAV8. *Mol. Ther.* 14, 45–53.
- Gulick, J., Subramaniam, A., Neumann, J., and Robbins, J. (1991). Isolation and characterization of the mouse cardiac myosin heavy chain genes. *J. Biol. Chem.* 266, 9180–9185.
- Su, H., Joho, S., Huang, Y., Barcena, A., Arakawa-Hoyt, J., Grossman, W., and Kan, Y.W. (2004). Adeno-associated viral vector delivers cardiac-specific and hypoxia-inducible VEGF expression in ischemic mouse hearts. *Proc. Natl. Acad. Sci. USA* 101, 16280–16285.
- Wang, G., Yeh, H.L., and Lin, J.J. (1994). Characterization of cis-regulating elements and trans-activating factors of the rat cardiac troponin T gene. *J. Biol. Chem.* 269, 30595–30603.
- Lee, C.J., Fan, X., Guo, X., and Medin, J.A. (2011). Promoter-specific lentivectors for long-term, cardiac-directed therapy of Fabry disease. *J. Cardiol.* 57, 115–122.
- Pacak, C.A., Sakai, Y., Thattaliyath, B.D., Mah, C.S., and Byrne, B.J. (2008). Tissue specific promoters improve specificity of AAV9 mediated transgene expression following intra-vascular gene delivery in neonatal mice. *Genet. Vaccines Ther.* 6, 13.
- Müller, O.J., Leuchs, B., Pleger, S.T., Grimm, D., Franz, W.-M., Katus, H.A., and Kleinschmidt, J.A. (2006). Improved cardiac gene transfer by transcriptional and transductional targeting of adeno-associated viral vectors. *Cardiovasc. Res.* 70, 70–78.

13. Rincon, M.Y., Sarcar, S., Danso-Abeam, D., Keyaerts, M., Matrai, J., Samara-Kuko, E., Acosta-Sanchez, A., Athanasopoulos, T., Dickson, G., Lahoutte, T., et al. (2015). Genome-wide computational analysis reveals cardiomyocyte-specific transcriptional Cis-regulatory motifs that enable efficient cardiac gene therapy. *Mol. Ther.* *23*, 43–52.
14. Selbach, M., Schwanhäusser, B., Thierfelder, N., Fang, Z., Khanin, R., and Rajewsky, N. (2008). Widespread changes in protein synthesis induced by microRNAs. *Nature* *455*, 58–63.
15. Brown, B.D., Gentner, B., Cantore, A., Colleoni, S., Amendola, M., Zingale, A., Baccarini, A., Lazzari, G., Galli, C., and Naldini, L. (2007). Endogenous microRNA can be broadly exploited to regulate transgene expression according to tissue, lineage and differentiation state. *Nat. Biotechnol.* *25*, 1457–1467.
16. Dhungel, B., Ramlogan-Steel, C.A., and Steel, J.C. (2018). Synergistic and independent action of endogenous microRNAs 122a and 199a for post-transcriptional liver detargeting of gene vectors. *Sci. Rep.* *8*, 15539.
17. Brown, B.D., Venneri, M.A., Zingale, A., Sergi, L., and Naldini, L. (2006). Endogenous microRNA regulation suppresses transgene expression in hematopoietic lineages and enables stable gene transfer. *Nat. Med.* *12*, 585–591.
18. Brown, B.D., Cantore, A., Annoni, A., Sergi, L.S., Lombardo, A., Della Valle, P., D'Angelo, A., and Naldini, L. (2007). A microRNA-regulated lentiviral vector mediates stable correction of hemophilia B mice. *Blood* *110*, 4144–4152.
19. Keaveney, M.K., Tseng, H.A., Ta, T.L., Gritton, H.J., Man, H.-Y., and Han, X. (2018). A MicroRNA-Based Gene-Targeting Tool for Virally Labeling Interneurons in the Rodent Cortex. *Cell Rep.* *24*, 294–303.
20. Geisler, A., Schön, C., Größl, T., Pinkert, S., Stein, E.A., Kurreck, J., Vetter, R., and Fechner, H. (2013). Application of mutated miR-206 target sites enables skeletal muscle-specific silencing of transgene expression of cardiotropic AAV9 vectors. *Mol. Ther.* *21*, 924–933.
21. Hinkel, R., Lange, P., Petersen, B., Gottlieb, E., Ng, J.K.M., Finger, S., Horstkotte, J., Lee, S., Thormann, M., Knorr, M., et al. (2015). Heme Oxygenase-1 Gene Therapy Provides Cardioprotection Via Control of Post-Ischemic Inflammation: An Experimental Study in a Pre-Clinical Pig Model. *J. Am. Coll. Cardiol.* *66*, 154–165.
22. Otterbein, L.E., Foresti, R., and Motterlini, R. (2016). Heme Oxygenase-1 and Carbon Monoxide in the Heart: The Balancing Act Between Danger Signaling and Pro-Survival. *Circ. Res.* *118*, 1940–1959.
23. Tomczyk, M., Kraszewska, I., Szade, K., Bukowska-Strakova, K., Meloni, M., Jozkowicz, A., Dulak, J., and Jazwa, A. (2017). Splenic Ly6C<sup>hi</sup> monocytes contribute to adverse late post-ischemic left ventricular remodeling in heme oxygenase-1 deficient mice. *Basic Res. Cardiol.* *112*, 39.
24. Lagos-Quintana, M., Rauhut, R., Yalcin, A., Meyer, J., Lendeckel, W., and Tuschl, T. (2002). Identification of tissue-specific microRNAs from mouse. *Curr. Biol.* *12*, 735–739.
25. Landgraf, P., Rusu, M., Sheridan, R., Sewer, A., Iovino, N., Aravin, A., Pfeffer, S., Rice, A., Kamphorst, A.O., Landthaler, M., et al. (2007). A mammalian microRNA expression atlas based on small RNA library sequencing. *Cell* *129*, 1401–1414.
26. Kitamuro, T., Takahashi, K., Ogawa, K., Udono-Fujimori, R., Takeda, K., Furuyama, K., Nakayama, M., Sun, J., Fujita, H., Hida, W., et al. (2003). Bach1 functions as a hypoxia-inducible repressor for the heme oxygenase-1 gene in human cells. *J. Biol. Chem.* *278*, 9125–9133.
27. Guo, L., Zhang, Q., Ma, X., Wang, J., and Liang, T. (2017). miRNA and mRNA expression analysis reveals potential sex-biased miRNA expression. *Sci. Rep.* *7*, 39812.
28. Qiao, C., Yuan, Z., Li, J., He, B., Zheng, H., Mayer, C., Li, J., and Xiao, X. (2011). Liver-specific microRNA-122 target sequences incorporated in AAV vectors efficiently inhibit transgene expression in the liver. *Gene Ther.* *18*, 403–410.
29. Geisler, A., Jungmann, A., Kurreck, J., Poller, W., Katus, H.A., Vetter, R., Fechner, H., and Müller, O.J. (2011). microRNA122-regulated transgene expression increases specificity of cardiac gene transfer upon intravenous delivery of AAV9 vectors. *Gene Ther.* *18*, 199–209.
30. Li, Z.-Y., Xi, Y., Zhu, W.-N., Zeng, C., Zhang, Z.-Q., Guo, Z.-C., Hao, D.L., Liu, G., Feng, L., Chen, H.Z., et al. (2011). Positive regulation of hepatic miR-122 expression by HNF4 $\alpha$ . *J. Hepatol.* *55*, 602–611.
31. Coulouarn, C., Factor, V.M., Andersen, J.B., Durkin, M.E., and Thorgerisson, S.S. (2009). Loss of miR-122 expression in liver cancer correlates with suppression of the hepatic phenotype and gain of metastatic properties. *Oncogene* *28*, 3526–3536.
32. Burridge, P.W., Keller, G., Gold, J.D., and Wu, J.C. (2012). Production of de novo cardiomyocytes: human pluripotent stem cell differentiation and direct reprogramming. *Cell Stem Cell* *10*, 16–28.
33. Mercola, M., Ruiz-Lozano, P., and Schneider, M.D. (2011). Cardiac muscle regeneration: lessons from development. *Genes Dev.* *25*, 299–309.
34. Shen, S., Bryant, K.D., Brown, S.M., Randell, S.H., and Asokan, A. (2011). Terminal N-linked galactose is the primary receptor for adeno-associated virus 9. *J. Biol. Chem.* *286*, 13532–13540.
35. Boisgerault, F., and Mingozzi, F. (2015). The Skeletal Muscle Environment and Its Role in Immunity and Tolerance to AAV Vector-Mediated Gene Transfer. *Curr. Gene Ther.* *15*, 381–394.
36. Mingozzi, F., Liu, Y.L., Dobrzynski, E., Kaufhold, A., Liu, J.H., Wang, Y., Arruda, V.R., High, K.A., and Herzog, R.W. (2003). Induction of immune tolerance to coagulation factor IX antigen by in vivo hepatic gene transfer. *J. Clin. Invest.* *111*, 1347–1356.
37. Mendell, J.R., Campbell, K., Rodino-Klapac, L., Sahenk, Z., Shilling, C., Lewis, S., Bowles, D., Gray, S., Li, C., Galloway, G., et al. (2010). Dystrophin immunity in Duchenne's muscular dystrophy. *N. Engl. J. Med.* *363*, 1429–1437.
38. Carpentier, M., Lorain, S., Chappert, P., Lalfer, M., Hardet, R., Urbain, D., Peccate, C., Adriouch, S., Garcia, L., Davoust, J., and Gross, D.A. (2015). Intrinsic transgene immunogenicity gears CD8(+) T-cell priming after rAAV-mediated muscle gene transfer. *Mol. Ther.* *23*, 697–706.
39. Lee, L.R., Peacock, L., Lisowski, L., Little, D.G., Munns, C.F., and Schindeler, A. (2019). Targeting Adeno-Associated Virus Vectors for Local Delivery to Fractures and Systemic Delivery to the Skeleton. *Mol. Ther. Methods Clin. Dev.* *15*, 101–111.
40. Doench, J.G., and Sharp, P.A. (2004). Specificity of microRNA target selection in translational repression. *Genes Dev.* *18*, 504–511.
41. Grimson, A., Farh, K.K., Johnston, W.K., Garrett-Engle, P., Lim, L.P., and Bartel, D.P. (2007). MicroRNA targeting specificity in mammals: determinants beyond seed pairing. *Mol. Cell* *27*, 91–105.
42. Jopling, C. (2012). Liver-specific microRNA-122: Biogenesis and function. *RNA Biol.* *9*, 137–142.
43. Gao, W., He, H.-W., Wang, Z.-M., Zhao, H., Lian, X.-Q., Wang, Y.-S., Zhu, J., Yan, J.J., Zhang, D.G., Yang, Z.J., and Wang, L.S. (2012). Plasma levels of lipometabolism-related miR-122 and miR-370 are increased in patients with hyperlipidemia and associated with coronary artery disease. *Lipids Health Dis.* *11*, 55.
44. Wang, S.-S., Wu, L.-J., Li, J.-H., Xiao, H.-B., He, Y., and Yan, Y.-X. (2018). A meta-analysis of dysregulated miRNAs in coronary heart disease. *Life Sci.* *215*, 170–181.
45. Zhang, X., and Jing, W. (2018). Upregulation of miR-122 is associated with cardiomyocyte apoptosis in atrial fibrillation. *Mol. Med. Rep.* *18*, 1745–1751.
46. Zhang, Z.W., Li, H., Chen, S.S., Li, Y., Cui, Z.Y., and Ma, J. (2017). MicroRNA-122 regulates caspase-8 and promotes the apoptosis of mouse cardiomyocytes. *Braz. J. Med. Biol. Res.* *50*, e5760.
47. Liang, W., Guo, J., Li, J., Bai, C., and Dong, Y. (2016). Downregulation of miR-122 attenuates hypoxia/reoxygenation (H/R)-induced myocardial cell apoptosis by upregulating GATA-4. *Biochem. Biophys. Res. Commun.* *478*, 1416–1422.
48. Karakikes, I., Ameen, M., Termglinchan, V., and Wu, J.C. (2015). Human induced pluripotent stem cell-derived cardiomyocytes: insights into molecular, cellular, and functional phenotypes. *Circ. Res.* *117*, 80–88.
49. Murry, C.E., and MacLellan, W.R. (2020). Stem cells and the heart—the road ahead. *Science* *367*, 854–855.
50. Ma, J., Guo, L., Fiene, S.J., Anson, B.D., Thomson, J.A., Kamp, T.J., Kolaja, K.L., Swanson, B.J., and January, C.T. (2011). High purity human-induced pluripotent stem cell-derived cardiomyocytes: electrophysiological properties of action potentials and ionic currents. *Am. J. Physiol. Heart Circ. Physiol.* *301*, H2006–H2017.
51. Gherghiceanu, M., Barad, L., Novak, A., Reiter, I., Itskovitz-Eldor, J., Binah, O., and Popescu, L.M. (2011). Cardiomyocytes derived from human embryonic and

- induced pluripotent stem cells: comparative ultrastructure. *J. Cell. Mol. Med.* *15*, 2539–2551.
52. Kuppasamy, K.T., Jones, D.C., Sperber, H., Madan, A., Fischer, K.A., Rodriguez, M.L., Pabon, L., Zhu, W.Z., Tulloch, N.L., Yang, X., et al. (2015). Let-7 family of microRNA is required for maturation and adult-like metabolism in stem cell-derived cardiomyocytes. *Proc. Natl. Acad. Sci. USA* *112*, E2785–E2794.
53. Portiér, G.L., Benders, A.G., Oosterhof, A., Veerkamp, J.H., and van Kuppevelt, T.H. (1999). Differentiation markers of mouse C2C12 and rat L6 myogenic cell lines and the effect of the differentiation medium. *In Vitro Cell. Dev. Biol. Anim.* *35*, 219–227.
54. Stepniewski, J., Pacholczak, T., Skrzypczyk, A., Ciesla, M., Szade, A., Szade, K., Bidanel, R., Langrzyk, A., Grochowski, R., Vandermeeren, F., et al. (2018). Heme oxygenase-1 affects generation and spontaneous cardiac differentiation of induced pluripotent stem cells. *IUBMB Life* *70*, 129–142.
55. Lian, X., Zhang, J., Azarin, S.M., Zhu, K., Hazeltine, L.B., Bao, X., Hsiao, C., Kamp, T.J., and Palecek, S.P. (2013). Directed cardiomyocyte differentiation from human pluripotent stem cells by modulating Wnt/ $\beta$ -catenin signaling under fully defined conditions. *Nat. Protoc.* *8*, 162–175.